Journal of Thermal Analysis, 47 (1996) 151-163

PREDICTABLE BEHAVIOR OF SMART MATERIALS (Cu–Zn–Al SMA)

A. Isalgue, H. Tachoire, A. Torralba, V. R. Torra and V. Torra***

CIRG–DFA–ETSECCPB, Polytechnic University of Catalonia, Campus Nord B–4, E–08034 Barcelona, Spain

Abstract

Reliability is a critical word in industrial applications of Shape Memory Alloys. Accurate and reproducible transformation hysteresis cycles and internal loops were obtained in single crystals using a high resolution automatized equipment. From a mechanical model formulated for a single martensite plate, the shape of the hysteresis cycle is obtained by generalizing the representation to N plates. The observed time effects on the hysteresis loops related to diffusion processes were also taken into account. It allows to explain the martensite recoverable creep and the micromemory effects. Also, the room temperature effects on the parent phase (for instance, summer to winter) acting over the transformation temperature are quantified.

Keywords: modelling, shape memory alloys, thermal analysis, thermomechanical equipment, time effects

Introduction

Cu–Zn–Al alloys [1] belong to the so-called smart materials [2], due to the shape memory effect (one way and two ways) and the pseudoelasticity. Potential applications [3] of these materials require a rigorous stability of the transformation temperatures and a small hysteresis. The applications of the SMA to the continuous actuators involve a time guarantee about the constructed devices related to the suitable composition and heat treatment. Reliability is a critical word in industrial applications of SMA. The industrial interest needs an experimental method classifying the available alloys. Technical application of the continuous actuator implies some tens of thousand's of complete or partial cycles in several years. The design and construction [4] of shape memory alloys (SMA) devices can be greatly improved if models are developed for the description of the behavior of the material in the stress, strain, temperature (σ, ε, T) coordinate system. These models, which are time independent and obviously do

* Permanent address: Lab. Thermochimie, Univ. de Provence, F-13331 Marseille CEDEX 03, France
**Author to whom all correspondence should be addressed.

0368–4466/96/ $ 5.00

John Wiley & Sons, Limited
Chichester

not take into account the irreversible actions of the external fields and internal irregularities (like grain boundaries), are the basis to include the observed time effects. For instance, the martensite recoverable creep, the stress evolution at constant strain and the micromemory.

Using an adapted instrumentation with improved resolution [5–7] (differential and nondifferential conduction calorimeter, thermomechanical equipment's and resistance measurements) permits an evaluation of the irreversible evolution (like dislocation creation), the time evolution of the samples with or without cycling, and the relevant parameters characterizing the properties of the alloys. Accurate and reproducible transformation hysteresis cycles with internal loops were obtained in single crystals [8–9]. They were interpreted in terms of elementary plates, for which a mechanical model was formulated (a spring including two types of friction: nucleation and interface friction) [9]. In general, the shape of the hysteresis cycle can be obtained by generalizing the representation to N plates. The observed time effects on the hysteresis loops related to diffusion processes (due to coexistence parent to martensite phases), were also taken into account. The equilibrium temperature T_0 and, eventually, its dependence with time, is decisive in simulation and, obviously, in practical applications. An extended time dependent model [10] was put forward, based on the observed elementary processes. It allows to explain the martensite recoverable creep, the micromemory effects, and to simulate with a good agreement the observed behavior.

In this work, the computerized high resolution thermal analysis set-up and the thermomechanical equipment are briefly described. The effects of the coexistence parent-martensite is analyzed and modeled (in stress, strain, temperature and time coordinates). Careful analysis of the room temperature (T_{RT}) effects on parent phase determines the long time evolution of the transformation temperatures. The particular effects connected to the yearly room temperature evolution are quantified and estimated.

Samples and instrumentation

Single crystals (Cu–Zn–Al) were used having an electron concentration of 1.48 e/a. The nominal transformation temperature is between 280 to 290 K. The samples were homogenized at 1123 K and, then, water or air quenched. The samples used in the stress-strain analysis were cut according to the appropriate crystallographic axis producing the maximum deformation during the transformation (near 9%).

The set of conditions imposed in carrying out the experiments suggests that the transformation should be analyzed so that the phenomena under study are separated (using sufficient resolution). For instance, in a single crystal, a temperature induced stress free transformation (parent to martensite) produces

several hundreds (or thousands) of domains in, around, twenty or more kelvin. Under constant stress, in the temperature induced transformation, the number of plates reduces but the associate temperature domain decreases accordingly. The remaining temperature domain is, probably, related with minor composition effects. The temperature resolution needed for a detailed description approaches 0.01 K. Then the temperature rate should be 0.01 K s^{-1} (or less) for a careful description of the whole transformation process and the total time elapsed easily overcomes 6 h.

The constructed equipment was based on the high resolution thermal analysis for microscopic analysis of the transformation (or thermomicroscopy) [5]. Figure 1 shows schematically the equipment. A water flow from an external thermostat (*e* and *e'*) as reference temperature permits via one Peltier plate (a), a working surface (a copper plate of 40×40 mm^2) with programmed temperature. A platinum resistance (b) determines the controlled temperature. The observation of the sample (c), via a microscope (d) can be stored in a video-magnetic tape and/or as digitalized images in an auxiliary computer for further study. A gentle flow of CO_2 (f) avoids water condensation.

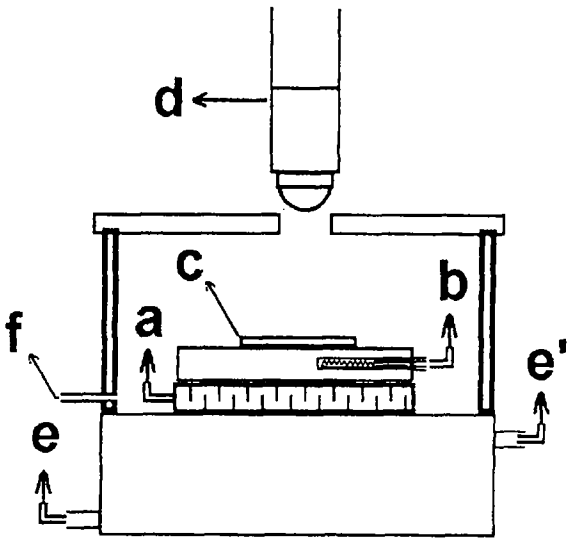

Fig. 1 Thermomicroscopy: thermal analysis of the transformation-retransformation process

The main computer ensures an appropriate feedback between the measured temperature and the DC current sent to the Peltier plate. The system works in the non-linear range. Calibration procedure implies the evaluation of the Peltier sensitivity S_p as a function of the expected temperature and, also, an evaluation of the dynamic parameters as the 'time constants' τ_i with a minor temperature dependence. The standard temperature control includes a 'classical' predictor-corrector scheme for the expected reproducibility (usually near 0.003 K).

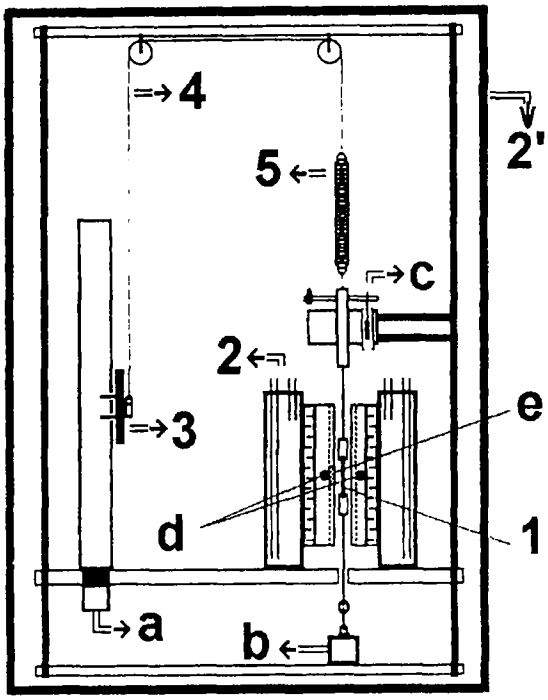

Fig. 2 Stress-strain-temperature high resolution equipment

Using two controlled temperature plates (120×40 mm^2) a stress-strain-temperature (and, eventually, time) equipment has been built [6]. The sample, usually with 25 mm in length and near 1 mm^2 in section (see 1 in Fig. 2) is situated on the center of two independent controlled plates. A liquid flow from an external thermostat determines the reference temperature used by the Peltier plates (2) and the protection chamber (2'). The computerized force control (a) establishes the vertical displacement (3) on the motorized system via a steel wire of the fishing type (4) changing the spring length (5) and the associated force. The system determines the force (b), the length (c), the temperatures (d) and, eventually, the energy dissipated by a Seebeck semiconductor plate (e). The equipment, completely computerized, operates between 285 to 365 K. The available resolution arounds 1 mN in force (full scale 20 or 200 *N*), 0.1 μm in lengthening (full scale 4 mm), 0.005 K in temperature and 1 s in time.

From the high resolution thermal analysis system a computer controlled equipment has been developed for resistance measurements using the 'four wire' method. The resolution and reproducibility in the temperature control and programation is around 0.005 K (Table 1). Copper wires are welded to the sample by standard Sn–Pb. To minimize the noise and parasitic e.m.f., an experimental point corresponds to 256 double readings using positive and nega-

Table 1 Experimental results at constant temperature (358.15 K). Time, resistance, standard deviation and associated fluctuations of the temperature. Measurements realized 15 months after the water quench

t/s	1	257	...	4609	4865	...	9907	10163
R/mΩ	2.50926	2.50925	...	2.50924	2.50931	...	2.50919	2.50932
$\Delta R/\mu\Omega$	0.20	0.18	...	0.18	0.21	...	0.15	0.18
ΔT/m*K*	2.5	–1.7	...	0.0	0.3	...	0.3	–0.8

tive DC current (near 0.20 A). The resistance value arounds 2mΩ, and the standard deviation for each point approaches 0.2μΩ (Table 1). Small oscillatory fluctuations ($\Delta R << 0.1$ μΩ) can be associated to the daily wave temperature influence. At constant temperature, the relative error $\Delta R/R$ was $0.5 \cdot 10^{-4}$ and the resistance measurement permits five significant figures. In this work, the used temperature limits are 260 and 373 K. Usually, the standard temperature rate in cycling was 20 mK s^{-1}. The temperature rate effects were analyzed and, for instance, the dR/dT increases if the dT/dt decreases (an effect related with the steady state effects on the sample).

Time independent behavior and modelling

By realizing cycles within the domain of the hysteresis curve, internal loops result (Fig. 3 left). It is clear that is not possible to assign to the points in these loops a single valued function of the experimental coordinates: stress, strain and temperature. When loading, the part 1–2 represents an increasing of the number of 'active' martensite plates or growing plates. Part 2–3 corresponds to a steady state: the same number coalesces and nucleates. In part 3–4 the number of active plates decreases as the transformation reaches the end of the available sample.

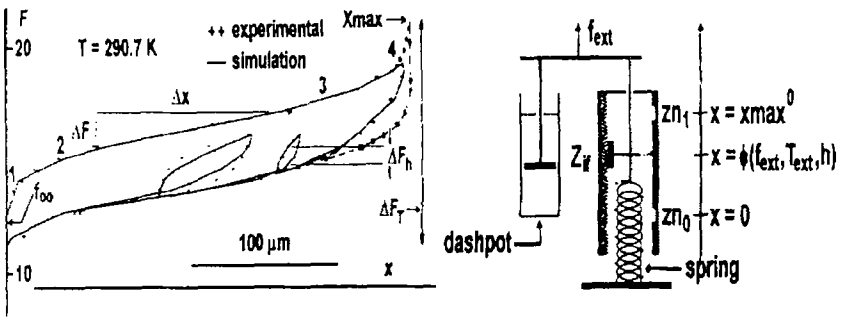

Fig. 3 Time independent processes; (left) force in *N vs.* lengthening at constant temperature in K, experimental and simulation; (right) mechanical analogy

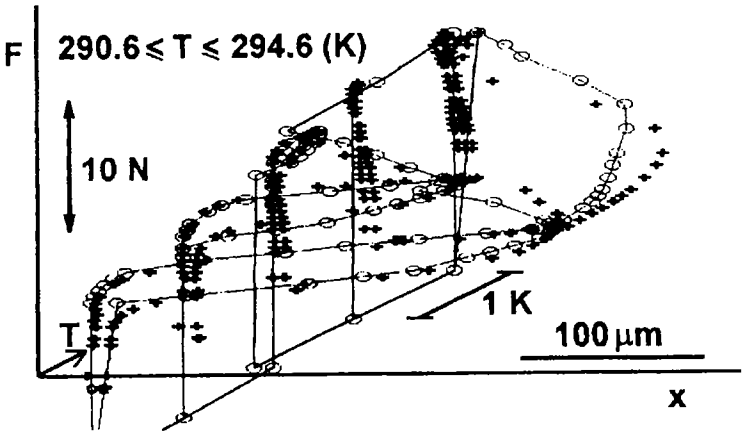

Fig. 4 Hysteretic behaviour and simulation in F–x–T coordinate space (+++ experimental, o–o–o calculated)

The maximum lengthening of the complete transformation is X_{max}; ΔF and Δx determines the mean slope in 'steady state' transformation process; ΔF_h corresponds to the minimal macroscopic hysteresis; ΔF_T to the mean slope of the transformation process and f_{oo} to the critical stress. From the experimental observations, it was found that the behavior of a single martensite plate [11–12] can be schematized including the nucleation of martensite, the nucleation of austenite or the decoalescence between two plates, the interface friction and the pseudoelasticity (as df/dx). Such behavior – for each martensite plate – can be well represented by the mechanical system depicted in Fig. 3 (right) derived from reference [13] which uses a spring with joined coils. This last condition explains the temperature dependence of the transformation stress: to a greater temperature corresponds a greater force joining the coils, following the Clausius-Clapeyron (CC) equation. The supplementary stress to overcome the temperature effect equals $(df/dT)_{CC}(T_{ext}-T_o)$. The model for a 'mean plate' (without microplate effects associated to the initial parts of growth) includes interface friction (z_{if}), intrinsic thermoelasticity (equivalent to the spring constant) and nucleation (zn_o and zn_1). The used maximal lengthening for each plate is $x\max^o$. The actual lengthening, x, is a function φ of the external force f_{ext}, the temperature T_{ext} together with previous state of the plate or history h. The dashpot ensures a smooth movement without mechanical oscillations. The model allows also the study of the hysteresis cycles under changes of stress and temperature in F–x–T coordinate space (Fig. 4) [14].

The main parameters of the model to be identified for an 'average martensite plate' from the macroscopic measurements (Fig. 3) are:

a) The representative plate number N, usually chosen to be ≤100 for easy of calculation.

b) The maximum sample lengthening X_{max}, which is directly deduced from the complete transformation curve (Fig. 3 left). The maximum lengthening of each plate is then defined as $x\max^{\circ}=X_{max}/N$.

c) The reversible critical stress, $f_{oo}^{(1)}$, associated to the appearance of the first plate at the external temperature T_{ext}. This critical stress is zero if $T_{ext}=T_o$, i.e. at the equilibrium temperature.

d) The average interface friction, z_{if} for each plate. The mean hysteresis is $2z_{if}$ (nucleation is not considered in this parameter). The interface friction is determined from the internal loops, $z_{if}\sim\Delta F_h$ (Fig. 3 left).

e) The nucleation: parent to martensite, zn_o, and martensite to parent zn_1. They are taken as $zn_o\approx zn_1\approx\alpha X_{max}$, being $\alpha=\Delta F/\Delta x$ from the 2–3 zone in Fig. 3 (left).

f) The pseudoelastic behavior or the slope (df/dx), equivalent to the Hooke law of the spring. It is obtained as $(df/dx)\approx\alpha N$.

g) The appearance of new plates, associated to the minor composition effects on the sample, is controlled by f_{rate}, defined as

$$f_{rate}=f_{oo}^{(i+1)}-f_{oo}^{(i)}$$

Usually, f_{rate} is assumed to be constant, then, for the i-th plate

$$f_{oo}^{(i)}=f_{oo}^{(1)}+(i-1)f_{rate}.$$

This parameter can be obtained from the relationship $\Delta f_T\approx Nf_{rate}+\alpha X_{max}$, where Δf_T is shown in Fig. 3 right.

h) The temperature dependence by the Clausius-Clapeyron equation $(df/dT)_{CC}$ or $(d\sigma/dT)_{CC}$. The CC equation establishes an equivalence between temperature and force effects and is taken as a change of the critical stress,

$$f_{oo}^{(1)}=(df/dT)_{CC}(T_{ext}-T_o)$$

i) Eventually, a new parameter can be introduced as an explanation of the intrinsic and nonsymmetric behavior during the appearance (by a microplate) and disappearance (without microplate) of each plate. The parameter quantifies the extreme situations: the minor overheating corresponding to the complete disappearance of the traces of the plates or the supplementary cooling associated to a complete 'coalescence'.

With this parameters, the transformation path for the i-th plate is considered by parts in order to evaluate the lengthening $x^{(i)}$ of the plate i. Previous to the nucleation:

$$f_{ext}<f_{oo}^{(i)}+zn_o+z_{if}\quad\text{and } x^{(i)}=0$$

At (below) the martensite nucleation

$$f_{ext} = f_{oo}^{(i)} + zn_o + z_{if} \quad \text{and } x^{(i)}=0$$

After the nucleation (increasing the martensite amount):

$$f_{ext} = f_{oo}^{(i)} + z_{if} + \left(\frac{df}{dx}\right) x^{(i)} \quad \text{and } x^{(i)} = x^{(i)}$$

At the end of the growth,

$$f_{ext} \geq f_{oo}^{(i)} + z_{if} + (df/dx)\, x\max^{o} \qquad \text{and } x^{(i)} = x\max^{o}$$

The remaining parts of the cycle are constructed in the same way. The initial parameters are determined from the experimental curve (Fig. 3 left). They allow the representation of the hysteretic behavior of a single crystal in the f, x, T space, by generalizing the model to N independent plates. The initial values are then improved using a technique based in the Marquard algorithm [15–16]. Attention is paid to the instabilities produced by the frictional contributions. The simulations presented in Figs 3 and 4 show the adequate prediction (time independent) obtained for different transformation cycles.

The parent martensite coexistence

In order to separate the different contributions associated to the coexistence of the austenitic and martensitic phases, further experiments were done. The first step was to obtain a quantitative approach to the 'martensite creep' (spon-

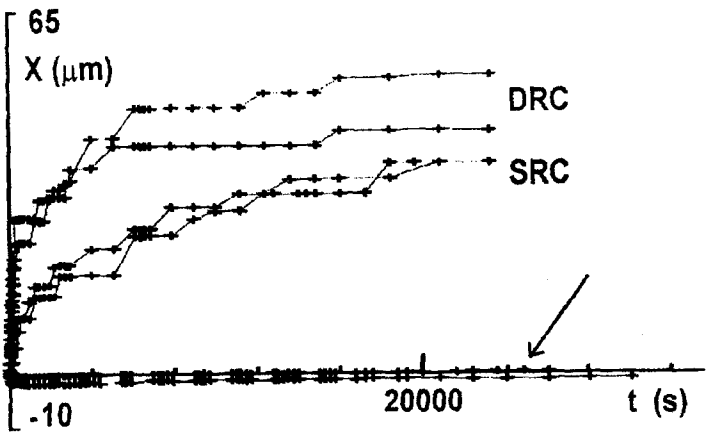

Fig. 5 Recoverable SRC and DRC effects: martensite lengthening *vs.* time (creep process at constant load)

taneous growth of martensite with time at constant stress and temperature in a partially transformed state). Experiments were carried out arriving to the initial point at a stress rate near zero (≤ 1 kPa s^{-1}). The creep against time is presented in Fig 5. This type of phenomenon is called 'Static Recoverable Creep' (SRC in Fig. 5) [10, 17]. The maximum lengthening obtained with SRC is, within the experimental scatter, the same in each point of the linear part of the transformation curve and lower outside. It is possible to relate this phenomenon to the coexistence of both phases (or equivalently to the presence of interfaces). The hysteresis cycle is locally deformed in the retransformation. This is classically known as micromemory. The normal shape of the hysteresis cycle is recovered after a few minutes in parent phase, but not instantaneously (the β-recovery process). The SRC effect during the unloading part of the hysteresis cycle is less marked and an initial small reduction of length can be detected, probably associated with the recovery of β in the neighborhood of the retransformed parts (see, the arrow in Fig. 5). The role that the barrier (interface friction) producing the hysteresis plays against the growth of the martensite, explains the reduced activity of the SRC on unloading. An increase in complexity is achieved by loading the material at relatively higher stress rates (1 kPa s^{-1} $\leq d\sigma/dt \leq 10$ kPa s^{-1}), which is called 'Dynamic Recoverable Creep' or DRC. The behavior is similar to SRC but more pronounced, as show in Fig. 5. In the par-

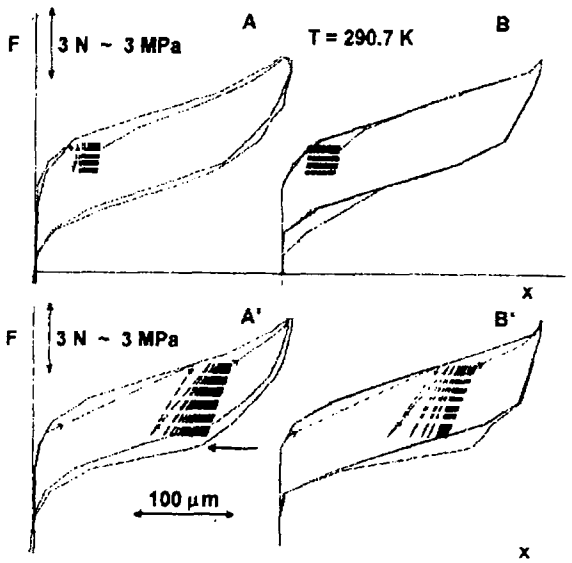

Fig. 6 Force *vs.* lengthening with internal loops using different width; A and A') experimental measurements; B and B') simulation. Each measurement includes an initial complete cycle, a partial load with a subsequent series of internal loops ended by a full load and a complete unload to the parent phase. Only extreme points are measured or calculated in internal loops. The arrow indicates the micromemory effect

ticular case of periodic oscillations (for instance, several internal loops) an important evolution exists, as it can be seen in Fig. 6 (A and A'). The results indicate that the zone of the material affected by the cycling (related to the range of forces used) tends rapidly to the martensitic state and eventually produce the transformation of neighboring plates. On unloading, a more important stabilization (or micromemory) is observed (see, for instance, the arrow in Fig. 6 A').

The macroscopic effects occurring in the transformation from parent to martensite are connected with local stabilization (increase of T_o) processes, activated by the existence of interfaces (SRC) and eventually their collective movement (DRC). The action of time over the system configuration is taken into account as an appropriate shift of the equilibrium temperature T_o of each affected plate (with parent to martensite coexistence).

The observation of SRC and DRC indicates an exponential behavior of x (Fig. 5) at least with one time constant. Transforming the x lenghtening in temperature changes using the Clausius-Clapeyron equation and the mean slope of the hysteresis cycle, the time constant and the associated equilibrium temperature changes are,

$$\tau_{SRC} \sim 9000 \text{ s} \qquad \Delta T_{o(SRC)} \sim 0.50 \text{ K}$$

$$\tau_{DRC} \sim 200 \text{ s} \qquad \Delta T_{o(DRC)} \sim 0.25 \text{ K}$$

In retransforming, the main action is associated to the β recovery process (local recovery of T_o). The time constant for this process is $\tau_\beta \sim 900$ s.

As a consequence of the previous results, time dependent contributions were added to the time independent model. The computer program (available on request) considers the material as formed by β domains which can transform partially or totally to martensite. From the equilibrium temperature and the previous configuration, the action of the external fields (force f_{ext} and temperature T_{ext}) is calculated for each time t_i using the Clausius-Clapeyron equation. The result is the lengthening of each domain and consequently the total length x_i. The iteration follows with the analysis of the new equilibrium temperatures for each plate. In the general case, the whole complex system will be simulated as a sum of the simpler SRC and, if appropriate, increased by DRC cases. The DRC approach is used if collective movement of interfaces parent/martensite exists over near neighboring plates. Most of the observed experimental results (if one avoids the creation of dislocations) can be explained with this model (Fig. 6 B and B'). Also, the evolution with time of T_o after a heat treatment (decreasing of the critical stress or equivalent increases of M_s) explains easily the appearance of an 'isothermal' transformation and also the difference between hysteresis cycles belonging to two distinct moments. Recoverable micromemory, independent of dislocation's creation, can be associated also to the local recoverable equilibrium temperature changes.

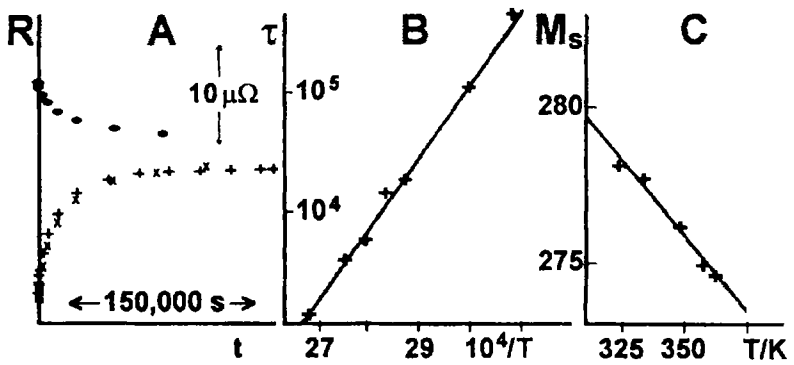

Fig. 7 A) Transitory effects on the resistance *vs.* time, working temperature 348 K from several previous situations; B) Logarithmic dependence of τ (in s) *vs.* $1/T$ (T in K); C) Measured values of M_s (in K) *vs.* the ageing temperature in parent phase

Ageing effects in parent phase and yearly effects on transformation temperature

After a temperature step, the resistance changes with time in exponential form (Fig. 7 A). Using the steady state measurements, the resistance shows a clear linear dependence against the temperature T_F in parent phase including the minor contribution of atomic order effects [18]. The time evolution of the resistance permits an approach to the main time constant (τ). For the analyzed temperatures (Fig. 7 B) the activation energy approach 1.2 eV. From the Fig. 7 B the value of the time constant at 298 K arounds $1.37 \cdot 10^7$ s (5 months). From the previous analysis, a temperature step at t_{ref} from T_{steady} to T induces a time evolution on M_s (Fig. 7 C) and the general form for an elapsed time $t-t_{ref}$, reads,

$$\Delta M_s = -0.11(T - T_{steady})$$

$$M_s(T, t) = M_s(T_{steady}, t = t_{ref}) + \Delta M_s \left[1 - e^{-(t - t_{ref})/\tau(T)}\right]$$

Table 2 Effect of a temperature step from T_{steady}=358.15 K to T. Effect on M_s after A h at the temperature T (B: experimental and C: calculated)

T/K	$A \equiv t-t_{ref}$/h	B: M_s/K	C: M_s/K
333.15	11.97	275.81	275.80
305.65	59.44	275.28	275.23
293.15	59.44	274.83	274.93

The Table 2 presents several predicted and experimental values after ageing at T_{steady} and subsequent A hours at T using the previous expressions. The effect of the summer and winter temperature (for instance, 298 and 283 K) produces extreme changes on the M_s near 1.6 K. The actual value of the M_s is smoothed by the effect of the associated time constant. As a working hypothesis, the effects can be related to the B2 order processes (near-neighboring atoms in parent bcc structure). A long time analysis and using aging at higher temperature (near 365 K) shows 'secondary' effects probably associated to the neighboring atoms (order $L2_1$).

Conclusion

The high resolution thermal analysis set-up (near 0.003 K) and derived equipments permits an excellent description of the SMA behavior. From high resolution experiments, some time independent parameters have been found, which allow to model SMA thermomechanical behavior. The characteristics of the hysteresis cycles of N plates in a single crystal single variant transformation can be identified and simulated by a computer using a physical approach in terms of intrinsic parameters: thermoelasticity, interface friction, nucleation processes (parent to martensite and vice versa) and the number of martensitic plates.

The observed time effects in gently cycling are connected with stabilization activated by the presence of interfaces, the recovery of the β phase and, eventually, the previous thermal treatments. They can be explained as a recoverable change of the equilibrium temperature T_o of each plate, allowing to interpret and to model the martensitic recoverable creep effects (increase of T_o) and micromemory (local change of T_o), as arising from changes of the atomic order accelerated by the coexistence of the phases.

The resistance measurements permits a quantitative approach to the temperature effects on parent phase. After a temperature step, the resistance changes with time in exponential form. Using the steady state measurements, the M_s shows a clear linear dependence against the ageing temperature T in parent phase. The effect of the summer and winter seasonal temperature produces changes on the M_s (around 2 K). The actual value of M_s is is smoothed by the effect of the associated time constant.

* * *

Research carried out under the project NATO 920452. Partial support from CICYT is gratefully acknowledged. V. T. acknowledges Dir. Pol. Terr. (Generalitat of Catalonia) for useful support. Fruitful discussions with Drs. F. C. Lovey and J. L. Pelegrina of CAB-Argentina (EEC-ALA/MED contract) are acknowledged.

References

1 L. Delaey in Material Science and Technology, Eds. R. W. Cahn et al., VCH, Weinheim, Germany, Vol. 5, 1991, p. 339.
2 C. M. Wayman, MRS Bulletin, 18 (1993) 49.
3 Proc. Comett Course, The Science and Technology of Shape Memory Alloys, Ed. V. Torra, Univ. Illes Balears, Palma de Mallorca, Spain, 1989.
4 E. Patoor and M. Berveiller, Les alliages à mémoire de forme, Hermes, Paris, France, 1990.
5 A. Amengual and V. Torra, J. Phys. E: Sci. Instrum, 22 (1989) 433.
6 A. Isalgue and V. Torra, Meas. Sci. Technol., 4 (1993) 456.
7 A. Amengual, A. Isalgue, F. Marco, H. Tachoire, V. Torra and V. R. Torra, J. Thermal Anal., 38 (1992) 583.
8 F. C. Lovey, A. Amengual, V. Torra and M. Ahlers, Phil. Mag., A 61 (1990) 159.
9 F. C. Lovey, A. Isalgue and V. Torra, Acta Metall. Mater., 40 (1992) 3389.
10 A. Isalgue, J. L. Pelegrina, A. Torralba, V. R. Torra and V. Torra, in Mechanics of Phase Transformations and Shape Memory Alloys, Eds. L. C. Brinson and B. Moran, ASME-AMD Vol. 189, New York 1994 , p. 71.
11 A. Amengual, F. Garcias, F. Marco, C. Segui and V. Torra, Acta Metall., 36 (1988) 2329.
12 A. Amengual, F. C. Lovey and V. Torra, Scripta Metall. Mater., 24 (1990) 2241.
13 B.-T. Chu in Critical Review of Thermodynamics, Ed. E. B. Stuart et al., Mono Book Corp., Baltimore, USA, 1970, p. 305.
14 V. Torra, Thermochim. Acta, 200 (1992) 413.
15 D. W. Marquardt, Appl. Math., 11 (1963) 431.
16 W. E. Wentworth, J. Chem. Educ., 42 (1965) 96 and 162.
17 J. L. Pelegrina, M. Rodriguez de Rivera, V. Torra and F. C. Lovey, Acta Metall. Mater., 43 (1995) 993.
18 A. Isalgue, F. C. Lovey, J. L. Pelegrina and V. Torra, J. Physique IV, 5 (1995) C8–853.